Surfaces and Interfaces 51 (2024) 104642

Contents lists available at ScienceDirect

Surfaces and Interfaces

journal homepage: www.sciencedirect.com/journal/surfaces-and-interfaces

Electronic states near surfaces and interfaces of β-Ga_2O_3 and κ-Ga_2O_3 epilayers investigated by surface photovoltage spectroscopy, photoconductivity and optical absorption

Th. Dittrich [a], A. Parisini [b,*], M. Pavesi [b], A. Baraldi [b], A. Sacchi [b], F. Mezzadri [c,d], P. Mazzolini [b,d], M. Bosi [d], L. Seravalli [d], A. Bosio [b], R. Fornari [b,d]

[a] Helmholtz Zentrum Berlin für Materialien und Energie GmbH, Schwarzschildstr. 8, 12489 Berlin, Germany
[b] University of Parma, Department of Mathematical, Physical and Computer Sciences, Parco Area delle Scienze 7/A, 43124, Parma, Italy
[c] University of Parma, Department of Chemistry, Life Sciences and Environmental Sustainability, Parco Area delle Scienze 17/A, 43124, Parma, Italy
[d] IMEM-CNR, Institute of Materials for Electronics and Magnetism, Parco Area delle Scienze 37/A, 43124, Parma, Italy

ARTICLE INFO

Keywords:
Transient surface photovoltage spectroscopy
Ultra-wide band gap semiconductors
β- and κ-Ga_2O_3 polymorphs
Photoelectrical investigation
Surface, bulk, and interface defects

ABSTRACT

Transient surface photovoltage (SPV) spectroscopy, optical absorption, and photoconductivity (PC) were applied to study electronic transitions in (-201) β-Ga_2O_3 and (001) κ-Ga_2O_3 epitaxial layers on c-plane sapphire substrates. SPV signals were distinguished for charge separation near the surface and near the layer/substrate interface. The bandgaps of β-Ga_2O_3 and κ-Ga_2O_3 epitaxial layers were found to be, respectively, about 4.75 and 4.79 eV from optical absorption measurements, about 4.8 and 4.9 eV from PC, and 4.65 and 4.9 (near the surface) from SPV measurements. Near the κ-Ga_2O_3 layer/substrate interface SPV instead gives a value of 4.75 eV, possibly related to the presence of an interlayer. Defect-related transitions with onset energies at about 4.5, 4.1, and 3.5 eV were observed along the whole β-Ga_2O_3 layer cross-section. In contrast, defects related to different transitions were differently distributed in κ-Ga_2O_3 epitaxial layers: transitions setting on at about 4.3 eV originate from defects uniformly distributed across the layer, while transitions starting at 2.4 eV and 1.7 eV were respectively connected with defects located near the surface or near the layer/substrate interface. The PC measurements at photo-excitation energy above the bandgap indicated that defect densities and recombination losses were much larger in κ-Ga_2O_3 than in β-Ga_2O_3.

1. Introduction

Ultra-wide band gap semiconductors are of great interest for applications in power electronics, solar blind detection of UV-C radiation, sensing and photovoltaics. Ga_2O_3 and related ternary alloys attracted great scientific and applied interest [1-3]. The monoclinic β phase of Ga_2O_3 is thermodynamically stable and by far the most investigated and applied for fabrication of devices. It exhibits a high Baliga figure of merit, high breakdown voltage and transparency [2] and, remarkably, it can be grown as bulk crystals from the melt, permitting the manufacture of substrates for homoepitaxy. However, its low crystallographic symmetry leads to significant anisotropy of some physical properties that could be challenging for device manufacturing. The other metastable polymorphs, α, κ (also referred as ε), γ, and δ, are also gaining increasing interest. Among them, the κ-phase (orthorhombic) is particularly attractive for its higher crystalline symmetry, thermal stability up to about 700 °C [4] and the predicted spontaneous polarization along the [001] direction [5], as the space group $Pna2_1$ is non-centrosymmetric therefore the lattice is polar. However, deposition on standard hexagonal or cubic substrates leads to the formation of 120° rotated nanosized columnar domains [6], with structural defects-mediated anisotropy of the electronic transport properties [7].

The physical properties of β-Ga_2O_3 have been widely investigated [8], but the study of the κ-phase is less advanced. It was reported that both polymorphs contain intrinsic defects, such as Ga and O vacancies and their complexes, that provide electronic states in the bandgap [9-11]. The accurate knowledge of the band structure and the understanding and control of defects play a key role in the device design and performance. Conventional methods to investigate electronic properties are transport measurements, optical, photoelectrical, and space charge

* Corresponding author.
E-mail address: antonella.parisini@unipr.it (A. Parisini).

https://doi.org/10.1016/j.surfin.2024.104642
Received 22 April 2024; Received in revised form 4 June 2024; Accepted 15 June 2024
Available online 19 June 2024

spectroscopies, each of them being particularly suitable to obtain information on specific electronic states or transitions, namely localized shallow and deep states, as well as extended states and on layers with different extrinsic/background doping levels. Space charge spectroscopies can provide qualitative and quantitative information about defect related transitions in Ga_2O_3 but demand well-defined electrical contacts. These techniques cannot be simply applied for the characterization of Ga_2O_3 epitaxial layers grown on insulating sapphire substrates. In such case, in-plane photocurrent investigation can give information on weakly conductive epitaxial layers, measuring the signal between lateral contacts. Surface photovoltage (SPV) techniques do not demand contact preparation and are sensitive to local charge separation depending, for example, on the extension of a space charge region [12,13]. Therefore, transient SPV spectroscopy [14,15] opens the opportunity to distinguish processes of charge separation at buried interfaces, for example, between semiconductor thin films and charge-selective contacts [16]. Recently, SPV techniques have been applied to characterization of electronic transitions in Ga_2O_3 crystals [17]. Furthermore, SPV measurements can be also performed on insulating substrates such as diamond [18].

This work presents a comparison of electronic transitions in β- and κ-Ga_2O_3 epitaxial layers grown by MOVPE (metal organic vapor phase epitaxy), with a special focus on the spatial distribution of defects connected with specific transitions. For this purpose, we combined complementary techniques providing information about optically detected transitions (optical absorption spectroscopy), transitions leading to transport of photo-generated charge carriers within the epitaxial layers (photocurrent spectroscopy, PC) and transitions detected by charge separation across the surface and film/substrate interface space charge regions (transient SPV spectroscopy). The potential of the latter investigation technique, which is much less affected by the overall sample thickness with respect to optical absorption and photocurrent spectroscopy, is highlighted for the study of Ga_2O_3 polymorphs.

2. Experimental

2.1. The investigated materials

Two nominally undoped Ga_2O_3 layers grown on sapphire substrates were studied in this work, a β-Ga_2O_3 (thickness of 170 nm) and a κ-Ga_2O_3 (thickness of about 770 nm). The thickness was determined by evaluating the interference fringes with a Jasco UV–vis V-530 spectrophotometer.

The layers were grown using a vertical metalorganic vapor phase epitaxial reactor (MOVPE, SMI Inc.), using trimethylgallium (TMG), ultrapure water (H_2O) for κ-Ga_2O_3 and 6 N purity O_2 for β-Ga_2O_3 as precursors. The use of two different oxidants was necessary to obtain layers of good quality for both polymorphs [19]. 700 sccm of Ar were used as carrier gas for each precursor line, while additional 1000 sccm of Ar were separately delivered through the reactor showerhead.

The deposition of the κ-Ga_2O_3 layer was performed at a substrate temperature T_g = 650 °C (determined with a thermocouple placed in proximity of the substrate holder), keeping a ratio of about 117 between the partial pressure of the VI element and the partial pressure of the III element and a growth rate of about 25 nm/min, Reactor pressure was set at 100 mbar. Such conditions ensure the stabilization of pure κ-Ga_2O_3 [20]. For the β-Ga_2O_3 layer the growth was performed at T_g = 800 °C with VI/III ratio of 2800 and a growth rate of about 7 nm/min. Both samples were grown for 30 min.

For both samples the TMG and the oxidant precursor (H_2O or O_2) flows were abruptly interrupted after the 30 min of deposition. The reactor was then kept at the growth temperature for 2 min, with only Ar gas flowing, about 10 min at 500 °C and the sample was finally cooled down to room temperature at an average rate of about 12 °C/min.

2.2. Surface photovoltage measured at the film surfaces and buried substrate/film interfaces

Ga_2O_3 is an intrinsically n-type semiconductor. Therefore, upwards band bending is expected in Ga_2O_3 epitaxial layers at the surface and at the Ga_2O_3 / sapphire interface (called interface in the following), although effects due to surface electron accumulation or depletion have been reported in β-phase [21]. In Ga_2O_3 epitaxial layers, separation of photo-generated charge carriers is dominated by drift across the space charge regions (SCRs) near the surface and near the interface (Fig. 1). The built-in electric fields have opposite direction for the SCRs near the surface and near the interface. Consequently, SPV signals caused by charge separation across the surface and interface SCRs have opposite signs and can be therefore distinguished. The sign of SPV signals caused by drift in a SCR is independent of the photo-generation mechanisms. As a result, band-to-band and defect related transitions can be detected with respect to charge separation across the surface or interface SCRs.

The sapphire substrate is transparent for photon energies below or near the bandgap of Ga_2O_3. Therefore, the samples for the SPV measurements were placed with the Ga_2O_3 epitaxial layer closer to the front electrode (front illumination) or with the substrate closer to the front electrode (illumination of the flipped sample, called rear illumination in the following). Consequently, positive SPV signals result from charge separation across the surface and interface SCRs under front and rear illumination, respectively. In contrast, negative SPV signals result from charge separation across the interface and surface SCRs under front illumination and rear illumination, respectively.

Photo-generation under illumination takes place within the whole Ga_2O_3 layer for absorption lengths longer than or close to the layer thickness. In this case, SPV signals are a superposition of positive and negative components. Positive and negative components in SPV signals can be caused, for example, by a defect state distributed over the whole Ga_2O_3 layer (E_{t1} in Fig. 1). In this case, positive and negative components in SPV signals can be well distinguished if band bending is different at the surface and interface and/or if relaxation times are different for charge separation across the surface and interface SCRs. Defect states can be distributed, for example, only near the interface of the Ga_2O_3 epitaxial layer (E_{t2} in Fig. 1). In this case, SPV signals are inverted in sign for measurements under front illumination and under illumination from the back side.

Measurements by transient SPV spectroscopy were performed in air with a perforated Au-coated front electrode and a charge amplifier (Elektronik Manufaktur Mahlsdorf, resolution time 7 ns). The stainless-steel sample holder served as the back electrode. The intensity of signals was calibrated with an ac-signal (1 V peak-to-peak) applied at the back electrode. Samples were illuminated with pulses of a tunable Nd:YAG laser (EKSPLA, NT230–50) through the perforated front electrode. The laser was equipped with a spectral cleaning unit. The photon energies of the laser pulses (duration time 3–5 ns) were varied between 0.8 and 5.8 eV in steps of 50 meV. The spectrum of the photon flux was adjusted with a variable beam expander and a filter wheel. Fig. 2 shows the spectrum of the photon flux used in the measurements.

SPV transients were measured with an oscilloscope card (Gage, CSE 1600–4GS, sampling rate $2{\cdot}10^8$ samples/s). At each photon energy, ten transients were averaged at a repetition rate of 1 Hz. The amplification factor of the charge amplifier could be varied by changing the distance between the sample surface and the electrode. Home-made software was used for the spectral dependent logarithmic read-out of transients and plotting of contour plots (S. Fengler [15]). No SPV signals were detected for the polished stainless steel sample holder serving as the back electrode.

2.3. X-ray diffraction

X-ray diffraction was performed using a Thermo ARL X'TRA powder diffractometer equipped with a Thermo Electron solid state 0D detector

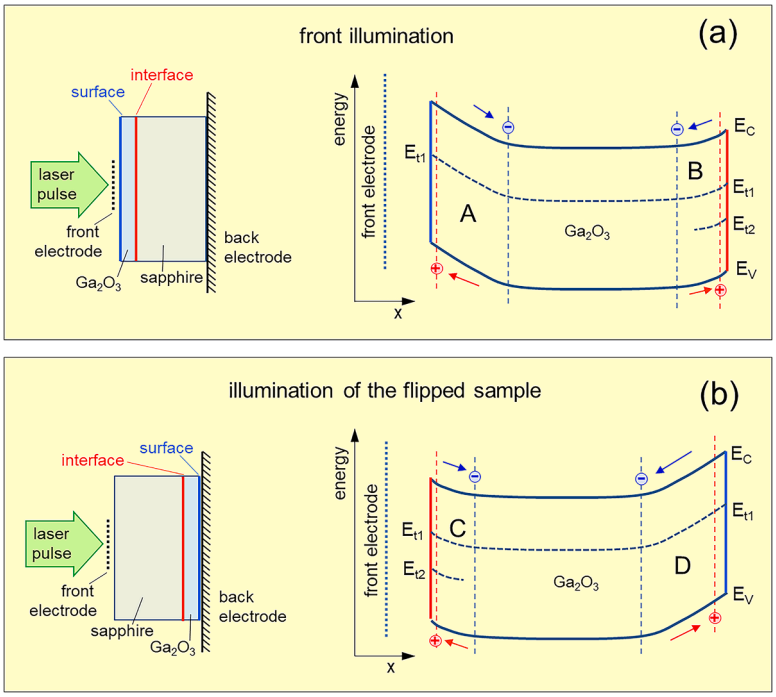

Fig. 1. Measurement arrangements (left) and schematic band diagrams (right) of a Ga_2O_3 epitaxial layer for SPV measurements under front illumination (a) and under illumination of the flipped sample (called rear illumination in the following) (b). A, B, correspond to charge separation across the surface and interface SCRs under front illumination while C, D represent charge separation at the interface and surface SCRs under rear illumination. The corresponding SPV signals have positive (A and C) and negative (B and D) signs. E_V, E_C, E_{t1} and E_{t2} denote the valence and conduction band edges and defect states distributed over the whole layer and only near the interface, respectively.

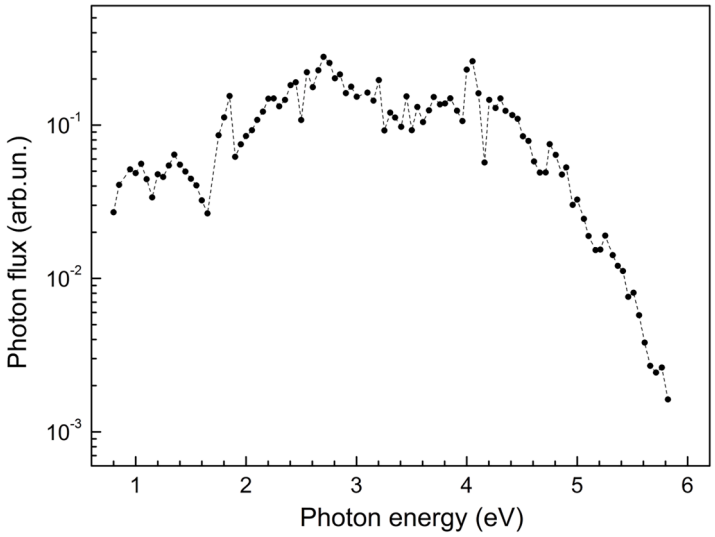

Fig. 2. Spectrum of the photon flux. The spectral dependent fluctuations in the photon flux are mainly caused by spectral dependent lateral inhomogeneity of the laser spot which cannot be compensated by the tunable beam expander.

making use of CuK_α radiation. The XRD analysis performed on the investigated samples highlights the presence of epitaxial single phase κ for the layer deposited at $T_g = 650$ °C and epitaxial single phase β for the one deposited at $T_g = 800$ °C (see Fig. 3**a** and 3**b**), as demonstrated by the sole presence of the (001) and (−201) families of peaks, respectively. The larger full width half maximum (FWHM) shown by the peaks of the β layer with respect to the κ one suggests lower thickness of the crystallites or/and higher strain. ω scans of the most intense reflections of the two polymorphs, i.e., (004) for κ-Ga_2O_3 and (−201) for β-Ga_2O_3 are reported in Fig. 3**c-d**. The FWHM of the rocking curves is 0.54 and 2.25° for the κ and β phases respectively, pointing out a higher mosaicity for the latter, likely ascribed to a poorer crystallinity, in agreement with the results of the 2θ-θ measurements.

2.4. Optical absorption and photoconductivity measurements

Transmission measurements were performed by means of a Varian 2390 UV–VIS-NIR double-beam spectrophotometer. A bare sapphire substrate was used as a reference. The transmission spectra were used to calculate the values of the absorption coefficient, and the interference fringes below the absorption edge were used to confirm the thicknesses of the Ga_2O_3 epitaxial layers.

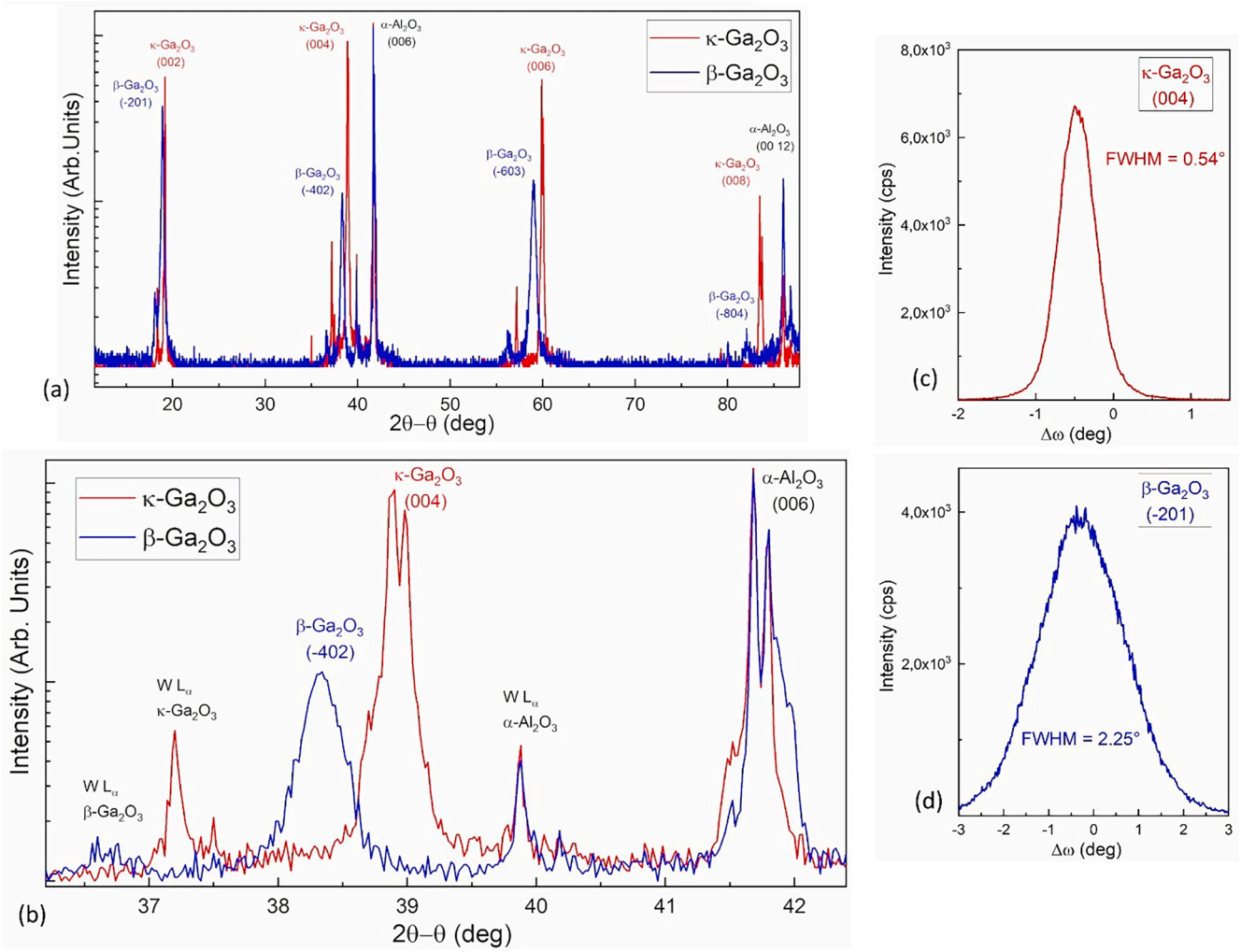

Fig. 3. (a) XRD 2θ-θ scan for the β and κ-Ga_2O_3 layer; (b) zoom over the range of interest for the (-402) and (004) reflections of the β and κ polymorphs, respectively; data reported in Log scale. (c) and (d): ω scans for reflections (004) of κ- and (−201) of β-Ga_2O_3. The relative full width half maximum (FWHM) values, obtained with a Pearson VII single peak fit, are reported.

One-face planar-geometry metal–semiconductor–metal structures were employed for the photoelectric characterization of Ga_2O_3 epitaxial layers. The ohmic contacts, consisting of Ti (20 nm) / Au (250 nm) bilayer, were deposited with a physical metal mask by sputtering (the geometry is described in Ref. [22]). The pattern is also adequate for the application of the Transfer Length Method (TLM) [11], then in the voltage range where the ohmic behavior of the electrical contacts was confirmed (a few tens of Volts), the dark resistivity measured at room temperature was about 3×10^6 Ωcm and 1×10^5 Ωcm, for the κ-Ga_2O_3 and β-Ga_2O_3 epitaxial layers, respectively. It can be observed that under light the current-voltage of the electrical contacts resulted linear in a wide range of applied voltages (see e.g. [9]). A Keithley Source-Meter Mod. 2400 was used for the current-voltage and photocurrent measurements.

The spectral photoresponse of the Ga_2O_3 epitaxial layers was acquired by illuminating the un-coated surface area between a pair of adjacent contacts (illuminated surface: width 200 μm, length 4000 μm) in air at room temperature. The experimental apparatus consisted of a light source system (ORIEL Mod. 66882) based on a 250 W halogen lamp suitably screened and focused, and a monochromator (CornerStone 130TM 1/8 m Mod. 74000) covering the range 200 - 650 nm with a wavelength resolution of 3 nm. The spectrum of the irradiance on the surface area between adjacent contacts was measured with a calibrated photodiode sensor (Newport 818 UV) and a correction factor was introduced for all the measured spectra. The voltage was maintained at 200 V during the photocurrent measurements.

3. Results

3.1. Optical and photo-current characteristics

Fig. 4 displays the absorption spectra of both κ- and β-phase Ga_2O_3 epitaxial layers. The two transmission spectra are quite similar with no significant differences between them. To obtain the value of the direct optical band gap from transmission measurements the standard Tauc method, i.e. the extrapolation of the square of the absorption coefficient to the energy axis, is often used. As previously reported [9], the standard Tauc plot in very thin samples can result in an overestimation of the optical band gap. This issue mainly arises when the hypotheses for the application of the method are not fulfilled [23]. In thin epitaxial layers, for instance, the non-parabolicity of the conduction band [24] may affect the linearity of the standard Tauc plot as the photon energies increase. Among the alternative methods [25-27] to estimate the optical band-gap, the fitting of the linear part of the absorption coefficient is exploited in this work. As shown in Fig. 4, the estimated optical bandgaps are in the range between 4.75 (β-Ga_2O_3) and 4.79 (κ-Ga_2O_3) eV, in agreement with data previously obtained on similar samples [9]. Incidentally, the absorption onsets in the absorption spectra start at

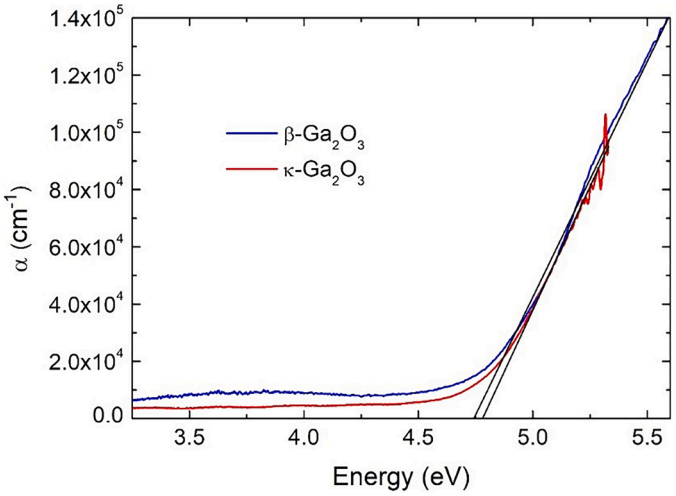

Fig. 4. Absorption spectra measured at RT for the β- and κ-Ga_2O_3 epitaxial layers. Straight lines are the fittings of the linear part of the absorption coefficients to estimate the optical bandgaps.

slightly lower energies in comparison to the fitted values that can be caused by impurity bands or other defect states near the band edges.

The responsivity spectra of κ-Ga_2O_3 and β-Ga_2O_3 epitaxial layers are compared in Fig. 5 on a semi-logarithmic scale. The spectral responsivity gives a quantitative evaluation of the photoconversion efficiency, and it represents the ratio between the photocurrent spectra and the absorbed optical power. The latter has been calculated from the incident optical irradiance, plotted in the inset of Fig. 5, taking into account the illuminated area between the considered pair of electrical contacts and the optical power really absorbed by the film. The Lambert-Beer's law allows to evaluate the absorbed optical power for each wavelength by considering the absorption coefficient, the thickness of the film and the incident spectral irradiance. The fractions of the incident power reflected by the surface of the Ga_2O_3 layer and by its interface with the substrate were estimated to be in the order of few percent. Both samples show similar trend with a maximum at photon energies above 5 eV, followed by a decrease in photoresponse at higher energies due to an increased influence of surface recombination when the penetration depth of light becomes comparable with the layer thickness. At the energy of the maximum, the photoconversion efficiency of the β-layer is about one order of magnitude higher with respect to the κ-layer, as the responsivity is the photocurrent normalized to the absorbed optical power. This result shows that the β-layer has the best transport properties, i.e. higher mobility-lifetime product, which in principle may derive from a lower recombination rate and/or higher photogain [22].

This experimental evidence should not be considered as a general statement about the potential of β and κ heteroepitaxial layers as active materials in photodetector devices, since the samples studied in this work differ in terms of synthesis parameters (e.g., gas carrier, precursors ratio) and were not optimized to maximize the photoresponsivity, but simply used for a thorough investigation of deep electronic states by multiple complementary characterization techniques.

Below 4.25 eV the responsivity of the κ-Ga_2O_3 epitaxial layer is larger in comparison to the β-Ga_2O_3 one, and the difference increases more and more by decreasing photon energy, until it reaches one order of magnitude at 2.5 eV; consequently, a better UV/VIS rejection ratio, of about 4 orders of magnitude, is evidenced in this β-phase sample. No sharp peaks are present below the bandgap energy in both samples and the smooth ripples at 4.0 eV and 4.5 eV can reasonably be traced back to the spectral profile of the incident optical power (see inset of Fig. 5). Excluding ripples, the behavior of spectral responsivity below the bandgap is approximately linear in semi-Log scale for the two samples, with different slopes. This could suggest the presence of a distribution of traps in the upper half of the bandgap even if the long response-time of the photocurrent observed in this material [22] can affect the spectral profile, resulting in a distorted trend, related to the elapsed time between two consecutive wavelengths compared to the photoresponse time. The features of the responsivity profiles should therefore be evaluated with some precaution. The photocurrent data were acquired starting from low to high photon energies (see arrow in Fig. 5) and this will be considered in the further discussion. The assignment of the maximum of responsivity to the energy gap transition clearly leads to an overestimation of this parameter. In addition, the appreciable shift of the maximum energy in the compared samples is evidence that the different response times have a different weight in the distortion of the spectral profile, higher in κ-sample. The lower persistence (related to the decay time) of the photocurrent in the β-sample could explain the more pronounced reduction of responsivity at energy higher than 5 eV, although that can also be related to a higher surface recombination. To give a more reliable estimation of the bandgap energy, the normalized responsivities of β-Ga_2O_3 and κ-Ga_2O_3 epitaxial layers are compared in Fig. 6 on a linear scale. The large difference in the slopes of the curves near the bandgap suggests that the extrapolation of the bandgap energy (dotted straight lines in Fig. 6) from them, as alternative approach, is not reliable, due to the long response time of the photocurrent, especially for κ-Ga_2O_3; in fact, this approach results in a large underestimation of the bandgap energy of the κ-sample.

A more reliable result can be achieved by considering the energy at

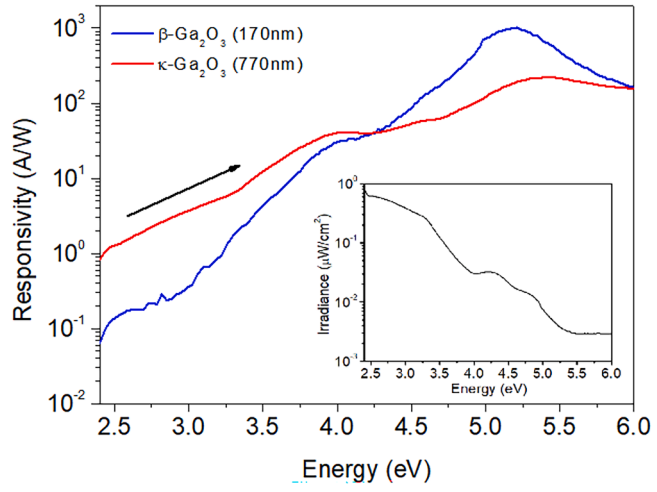

Fig. 5. Spectral responsivity of samples κ-phase (red line) and β-phase (blue line) in a semi-log scale. Insert: spectral irradiance on the surface of samples.

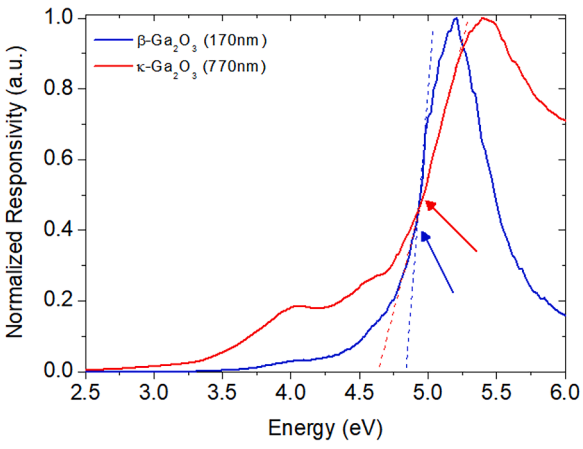

Fig. 6. Normalized spectral responsivity for the β- and κ-Ga_2O_3 epitaxial layers in a linear scale.

which a net change in slope of the signal occurs, which reflects the increase in the joint density of the states associated to the band-to band transition (indicated by the blue and red arrows). From this analysis, the photocurrent bandgap for β and κ samples results approximatively at 4.85 eV and 4.93 eV, respectively. Qualitatively, the slightly higher bandgap of the κ polymorph with respect to the β one agrees with previous first-principles theoretical calculations [28]. Incidentally, differences in the bandgaps obtained by different methods are expected since absorption measurements are sensitive to all optical transitions while photoconductivity and surface photovoltage measurements are sensitive only to those transitions leading to photogeneration and subsequent separation of mobile charge carriers. In addition, the regions tested by the various methods can be very different depending, for example, on distributions of carrier mobility and built-in electric fields.

Because of the highly defective nature of these investigated epitaxial layers, none of these techniques individually allows for an accurate evaluation of the bandgap width, but the comparison of results from multiple investigations may enable a more reliable assessment of the bandgap.

3.2. Characterization by SPV

3.2.1. SPV contour plots

Fig. 7 shows contour plots, i.e., the map of the SPV signals on logarithmic scales as function of logarithmic time and photon energy, for β-Ga_2O_3 and κ-Ga_2O_3 under front and rear illumination. Under strong absorption, i.e., at the highest photon energies, all SPV signals were positive. This means that the SPV signals were dominated by charge separation across the surface SCR under front and across the interface SCR under rear illumination.

For β-Ga_2O_3 under front illumination, the SPV signals were positive over the whole range of photon energies and times, i.e. the SPV signals were dominated by charge separation across the surface SCR. Furthermore, the SPV signals set on at about 3 eV and increased strongly from several mV to about 100 mV in the range between 4.6 and 4.8 eV. This means that SPV signals related to defect transitions were relatively small and that there was a well pronounced onset near the bandgap of β-Ga_2O_3. Furthermore, the SPV signals did not rapidly decay with time, i.e., relaxation of charge carriers separated in space was slower than about 0.1 s.

For β-Ga_2O_3 under rear illumination, negative and positive SPV signals were observed. Negative SPV signals between about 3 and 5 eV at times between the ns and μs ranges whereas the negative SPV signals did strongly increase between 4.6 and 4.8 eV. Positive SPV signals appeared at longer times. Therefore, relaxation of separated charge carriers was slower near the interface than near the surface. Furthermore, the positive SPV signals increased by about 1 order of magnitude around 4.2 eV. Therefore, charge separation across the surface SCR was much stronger than across the interface SCR for the β-Ga_2O_3 epitaxial layer, i.e. the band bending was larger for the surface SCR. A possible reason might be that the donor concentration was lower near the interface.

For κ-Ga_2O_3 under front illumination, negative SPV signals set on at photon energies below 1 eV and increased to tens of mV with increasing photon energy. This means that SPV signals related to deep defect states were dominated by charge separation across the interface SCR.

At photon energies above 2.5 eV, the sign of the SPV signals changed to positive at very long times whereas the time at which the sign changed to positive decreased with increasing photon energy towards about 0.1 ms at 4 eV. Therefore, SPV signals caused by a second band of deep defect states were dominated by charge separation across the surface SCR.

For κ-Ga_2O_3 under rear illumination, the SPV signals were positive over the whole spectral range at times shorter than 0.1 ms what gives additional evidence for strong charge separation from deep defect states across the interface SCR. Negative SPV signals appeared between about 4 and 4.7 eV at times longer than 0.1 ms and between about 3 and 4 eV at longer times changing from about 0.1 ms at 4 eV to tens of ms at 3 eV.

3.2.2. SPV analysis of transients

Fig. 8 shows typical SPV transients for a β-Ga_2O_3 epitaxial layer excited at 3.75, 4.61 and 5.71 eV under front and rear illumination. Under front illumination, the shapes of the transients were rather similar whereas the SPV signals appeared within the laser pulses, decreased during the following μs – 100 μs, depending on photon energy, increased

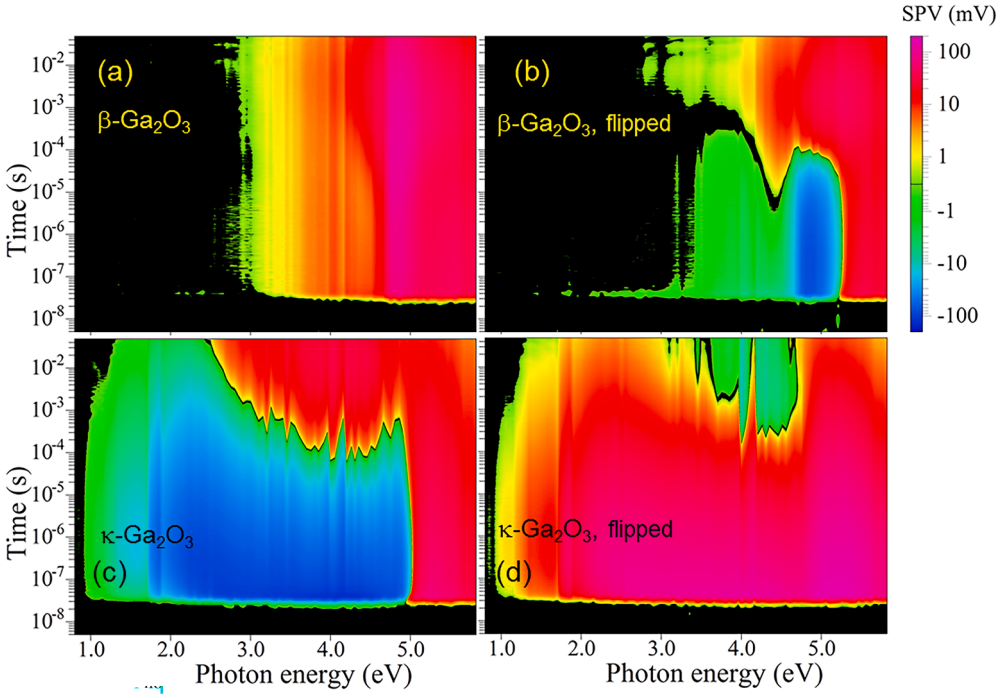

Fig. 7. Contour plots of β-Ga_2O_3 ((a) and (b)) and κ-Ga_2O_3 ((c) and (d)) epitaxial layers under front illumination ((a) and (c)) and under illumination of the flipped samples ((b) and (d)). The onset of the laser pulse was shifted to 20 ns in order to define a baseline on a logarithmic time scale.

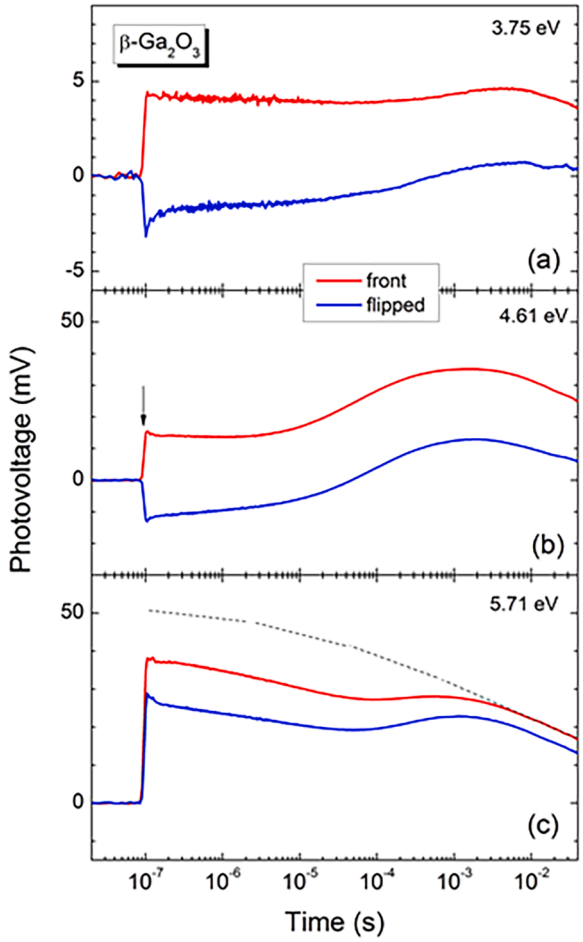

Fig. 8. SPV transients of β-Ga_2O_3 epitaxial layer under front and rear illumination (red and blue lines, respectively) for excitation at 3.75, 4.61 and 5.71 eV [(a) – (c), respectively]. The arrow in (b) marks the onset of the laser pulses. The dashed lines in (c) are guides for the eye to show the suitable shape of the positive component of the transient under front illumination as an example.

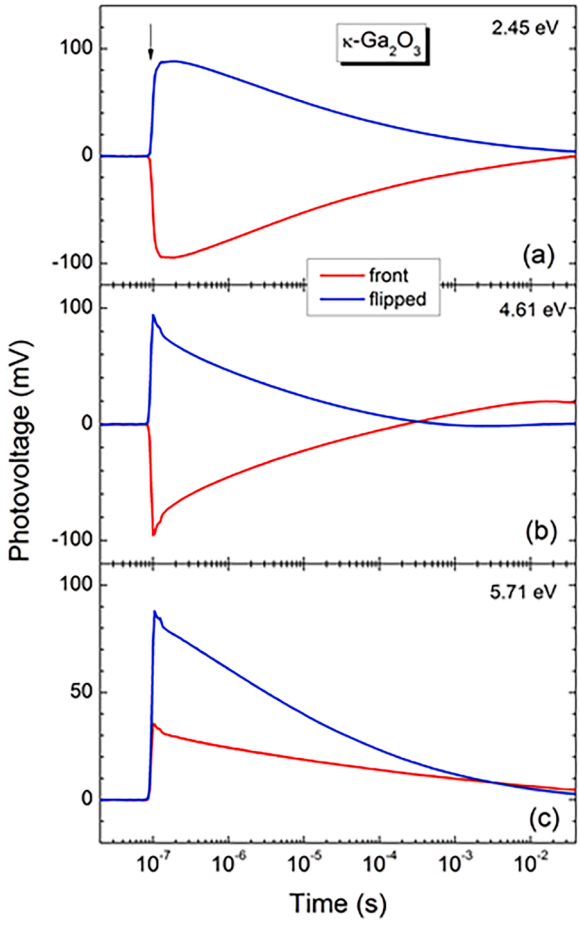

Fig. 9. SPV transients of κ-Ga_2O_3 epitaxial layer under front and rear illumination (red and blue lines, respectively lines) for excitation at 2.45, 4.61 and 5.71 eV [(a) – (c), respectively]. The arrow in (a) marks the onset of the laser pulses.

in the following time and started to decrease at times longer than millisecond(s). Under rear illumination, negative SPV signals appeared within the laser pulse for excitation at 3.75 and 4.61 eV. The negative SPV signals decreased slightly within the following 100 or 10 μs for excitation at 3.75 and 4.61 eV, respectively, decreased stronger and changed the sign to positive at longer times. Under rear illumination at 5.71 eV, the SPV transient was positive and very similar to the SPV transient obtained under front illumination at 5.71 eV.

The shapes of all SPV transients measured on a β-Ga_2O_3 epitaxial layer under front and rear illumination can be explained by a superposition of a positive and a negative SPV transient. Excitation at photon energies below the bandgap led to photo-generation across the whole β-Ga_2O_3 epitaxial layer. The fact that the SPV signals at short times changed the sign from positive to negative for changing from front to rear illumination provides evidence for stronger charge separation across the surface SCR than across the interface SCR.

Under excitation at 5.71 eV, the absorption length is shorter than the layer thickness, i.e., photo-generation is mainly limited to the SCR closer to the front electrode. The positive SPV signals at short times were larger under front than under rear illumination. This gives additional evidence for stronger charge separation across the surface SCR. Furthermore, the appearance of a superposition of positive and negative SPV transients under very strong absorption shows that photo-generation took partially place near the SCR closer to the back electrode.

Fig. 9 shows typical SPV transients for a κ-Ga_2O_3 epitaxial layer excited at 2.45, 4.61 and 5.71 eV under front and rear illumination. For excitation at 2.45 eV, the SPV signals were negative or positive over the whole time under front or rear illumination, respectively. This shows that charge separation occurred only across the interface SCR in the range of deep defects, i.e., that the vast majority of deep defects was concentrated near the interface. The SPV transients decayed to the half of the maximum within about 20 μs. Furthermore, the absolute values of the SPV signals were nearly identical under front or rear illumination, i.e., deep defect states were absent in the surface SCR.

For excitation at 4.61 eV under front or rear illumination, the SPV signals were negative or positive at shorter times, respectively, whereas the transients decayed to half of the maximum within few μs. At longer times, the sign of the transients changed. This gives evidence that some charge separation also occurred across the surface SCR and that the relaxation time was much longer than for charge separation across the interface SCR.

For excitation at 5.71 eV, the SPV signals were positive over the whole-time range under front and rear illumination, whereas the amplitude was much larger under rear illumination. Furthermore, there was no hint for any superposition of positive and negative SPV transients. Therefore, there was no photo-generation or diffusion of photo-generated charge carriers towards or near, respectively, the SCR closer to the back electrode, i.e., the diffusion length was much shorter than the thickness of the κ-Ga_2O_3 epitaxial layer.

SPV signals obtained under strong fundamental absorption directly after the onset of the laser pulses can be related to band bending. Incidentally, a precise value of the band bending in equilibrium could not be

obtained due to the fact that the SPV transients did only partially decay within the reciprocal repetition rate. All SPV signals measured directly after the onset of the laser pulses for excitation at, for example, 5.51 eV were positive and amounted to 46, 35, 58 and 140 mV for the β-Ga_2O_3 (front), β-Ga_2O_3 (rear), κ-Ga_2O_3 (front) and κ-Ga_2O_3 (rear) epitaxial layers, respectively. Therefore, the band banding was rather similar at the surface and interface for the β-Ga_2O_3 epitaxial layer. In contrast, the band bending was much higher at the interface than the one at the surface for the κ-Ga_2O_3 epitaxial layer that also correlated with the very high SPV signals caused by deep defects in the interface SCR.

3.2.3. SPV spectra

Fig. 10 shows SPV spectra for a β-Ga_2O_3 epitaxial layer which were obtained at 10 ns, 1 μs and 1 ms after the onset of the laser pulses under front and rear illumination. At first glance, transition energies can be related to onsets of changes in the slope whereas one has to keep in mind also the spectrum of the photon flux. Incidentally, a normalization to the photon flux, such as that usually done in photocurrent spectroscopy, is not useful for the analysis in transient SPV spectroscopy since there is an overlap of positive and negative SPV signals and since SPV signals are usually not proportional to the photon flux. The strongest change in the slope appeared as a strong increase of positive and negative SPV signals at 4.65 eV that corresponds to the bandgap of β-Ga_2O_3. A well pronounced increase at 4.65 eV was not observed in the spectrum of β-Ga_2O_3 extracted after 1 ms under front illumination.

The SPV signals set on around 3.5 eV in the spectra of β-Ga_2O_3 extracted after 10 ns and 1 μs and in the spectrum extracted after 1 ms under rear illumination. The increase of the SPV signals around 3.5 eV was extremely weak in the SPV spectra of β-Ga_2O_3 extracted after 1 ms under front illumination what correlated with the extremely weak signature at 4.65 eV in this spectrum.

A pronounced increase of positive and negative SPV signals appeared for β-Ga_2O_3 at 4.5 eV for spectra extracted after 10 ns and 1 μs. A signature related to the transition at 4.5 eV could not be observed in the spectrum of β-Ga_2O_3 extracted after 1 ms under front illumination. Furthermore, a transition at about 4.1 eV could be distinguished as an increase of SPV signals in the spectrum of β-Ga_2O_3 extracted after 1 ms under front illumination. In contrast, in the spectra of β-Ga_2O_3 extracted after 10 ns and 1 μs, a signature around 4.1 eV appeared as a little drop of SPV signals.

A steep decrease of SPV signals set on in the SPV spectra of β-Ga_2O_3 extracted after 10 ns and 1 μs under front illumination at photon energies above 4.8 - 4.9 eV and the SPV signals tended to increase again between 5.1 - 5.2 eV and about 5.6 eV. Under rear illumination, negative SPV signals extracted after 10 ns and 1 μs decreased above 4.9 eV, changed the sign to positive at about 5.2 eV and started to decrease above 5.6 eV in accordance with the strongly decreasing photon flux. The decrease of SPV signals above the bandgap and the following slight increase (front illumination) or change of sign (rear illumination) are caused by the superposition of SPV signals with opposite sign.

Fig. 11 shows SPV spectra for a κ-Ga_2O_3 epitaxial layer which were obtained at 10 ns, 1 μs and 1 ms after the onset of the laser pulses under front and rear illumination. The steepest increase of SPV signals towards more positive values set on at about 4.75 and 4.9 eV under front and rear illumination, respectively. This suggests the effective bandgap of κ-Ga_2O_3 to be about 4.9 and 4.75 eV for charge separation across the surface and interface SCR, respectively. This is a somewhat surprising finding that might be related to the very defective interface between Ga_2O_3 and the c-plane sapphire substrate, that was previously reported to lead to formation of a γ-Ga_2O_3 interlayer [6,29,31]. However, the

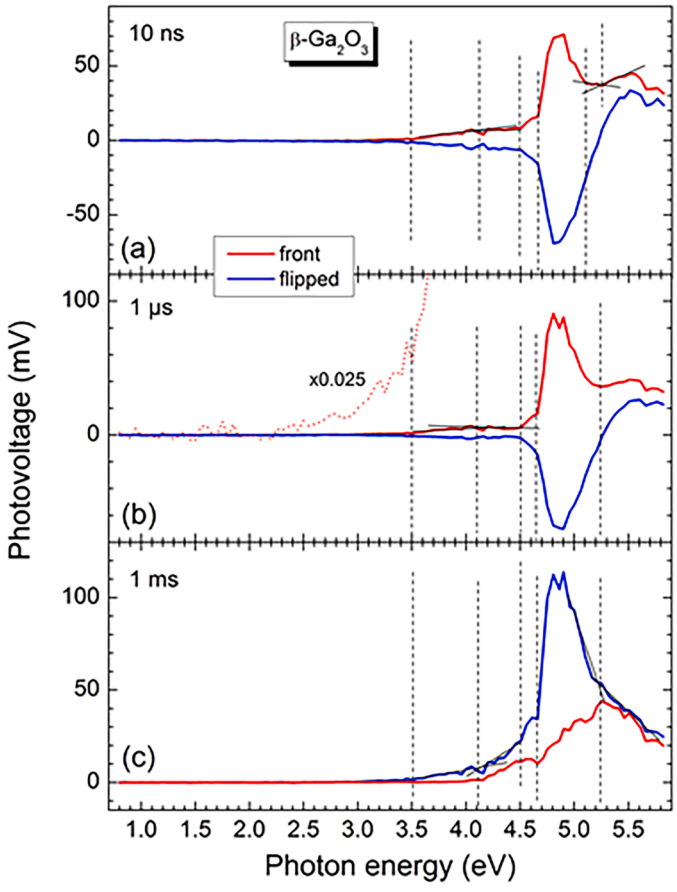

Fig. 10. SPV transients of β-Ga_2O_3 epitaxial layer under front and rear illumination (red and blue lines, respectively) extracted at 10 ns, 1 μs and 1 ms ((a) – (c), respectively). The solid and dashed black lines are for guiding the eye or mark electronic transitions, respectively.

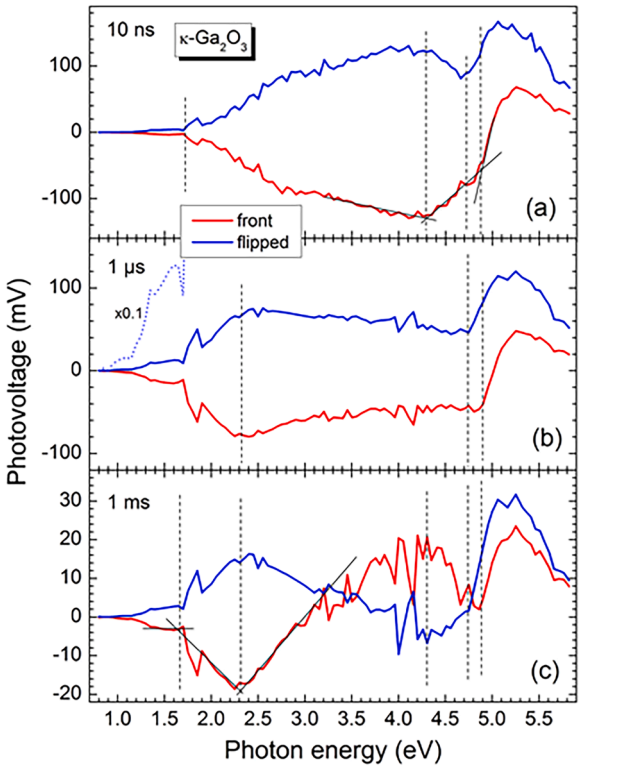

Fig. 11. SPV transients of κ-Ga_2O_3 epitaxial layer under front and rear illumination (red and blue lines, respectively) extracted at 10 ns, 1 μs and 1 ms ((a) – (c), respectively). The solid and dashed black lines are for guiding the eye or mark electronic transitions, respectively.

unambiguous assignment of the 4.75 eV transition to the γ-phase interlayer is not possible as SPV signals are sensitive to the interface region that includes the space charge region and extends well beyond the interlayer thickness.

Negative (front illumination) and positive (rear illumination) SPV signals set on above 1.1 - 1.2 eV and started to increase more steeply at about 1.7 eV for extraction at 10 ns, 1 μs and 1 ms. The related transitions were caused by defect states at the interface SCR. For extraction of the spectra at 1 μs and 1 ms, the SPV signals started to decrease at about 2.4 eV and even changed the sign at higher photon energies for extraction at 1 ms. Therefore, the related transition at 2.3 eV was caused by defect states at the surface SCR. Incidentally, the transition at about 2.3 eV could only be distinguished as a reduced increase of the SPV signals for extraction at 10 ns. Therefore, the relaxation of excited defect states was faster at the interface SCR.

The negative (front illumination) and positive (rear illumination) SPV signals of the spectra extracted at 10 ns decreased between about 4.3 eV and the onset of the effective bandgap of κ-Ga_2O_3. The decrease of the SPV signals is caused by the onset of SPV signals with opposite sign, i.e., as a signature of defect states leading to charge separation across the surface SCR. In contrast, the SPV signals between 4.3 eV and the effective bandgap changed in the opposite directions for the spectra extracted at 1 μs. Therefore, the related transition is a signature of defect states leading to charge separation across the interface SCR at longer times, i.e., the related defects are distributed over the whole κ-Ga_2O_3 epitaxial layer. The transition setting on at about 4.3 eV could not be distinguished in the spectra extracted at 1 μs, i.e., signals related to charge separation across the interface and surface SCRs compensated each other. This shows that the relaxation time related to charge separation via the transition at 4.3 eV was shorter for separation across the surface than across the interface SCR.

4. Discussions

The density of defects at the interface SCR of the κ-Ga_2O_3 epitaxial layer is high since defect related SPV signals are of the same order of the band-to-band transitions. It is reasonable to suppose that the band-to-band transitions of κ-Ga_2O_3 overlap with a high density of defects close to the valence and conduction band edges so that the effective bandgap is 4.75 eV. These results could be related to the formation of an interlayer (probably of γ phase), already observed by different research groups at the interface between κ-Ga_2O_3 and sapphire [6,29,30]. In this sense, it can be concluded that the value of the effective bandgap extracted for charge separation across the surface SCR corresponds to the bandgap of κ-Ga_2O_3 (4.9 eV). These values qualitatively agree with the bandgap evaluation of transmission and photocurrent measurements.

In SPV spectroscopy, transition energies can be assigned in general to an electron transition from the valence band into an un-occupied defect state or from an occupied defect state into the CB. A tentative overview of defect states compatible with the detected transitions is shown in Fig. 12.

In β-Ga_2O_3 (Fig. 12.**a**), a defect state at 4.5 eV below E_C of β-Ga_2O_3, responsible for the transition at 4.5 eV, was included. It is to be noted that a defect at 4.4 eV below E_C was reported in numerous literature reports. This result seems to be connected with the knee observed at about 4.3 eV by PC investigation, in correspondence of a clear signal increase. The transitions at about 4.1 and 3.5 eV in β-Ga_2O_3 could be related to defect states 4.1 or 0.55 and 3.5 or 1.15 eV, respectively, below E_C. There are no reports about defect states located at about 4.1 and 3.5 eV below E_C in literature, but there are reports about defect states in the range of 0.4 and 0.62 and in the range of 1.2 eV, respectively, below E_C. Therefore, we assume that the transition energies at 4.1 and 3.5 eV are related to defect states about 0.55 and 1.15 eV, respectively, below E_C in β-Ga_2O_3. In the case of β sample, the formation of few monolayers of α-Ga_2O_3 at the substrate/film interface is likely to occur

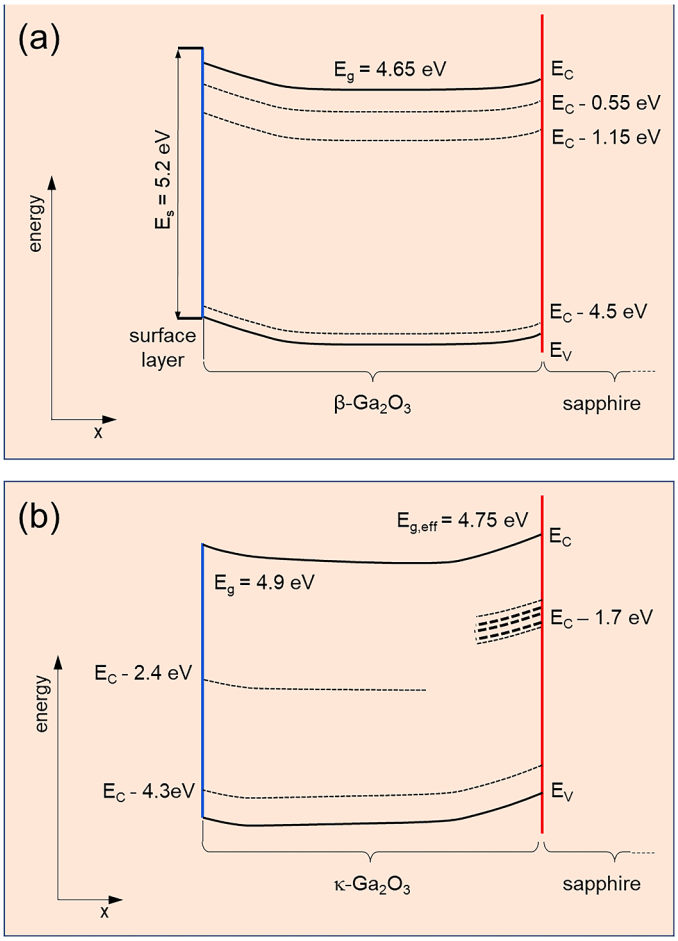

Fig. 12. Idealized band diagrams of β-Ga_2O_3 (a) and of κ-Ga_2O_3 (b), with indications of the deep electronic states deduced from the measurements with transient SPV spectroscopy.

as previously reported for deposition of (−201) β-Ga_2O_3 on c-oriented sapphire [32], However, since the photogeneration takes place over a much larger volume, the effect of this interlayer on SPV transients may be considered to be negligible.

In κ-Ga_2O_3 (Fig. 12.**b**), the defect transitions were rather different for charge separation across the surface SCR and across the interface SCR. Defect states with transition energies around 2.4 eV were observed for charge separation across the surface SCR. This feature is consistent with the main radiative emission detected by CL investigation [10], carried out on similar samples of κ-Ga_2O_3. The transition at 2.4 eV generally corresponds to the onset of a detectable PC signal, as observed in several samples (see e.g. [9,22]), where for increasing energy of the incident light the PC signal increases continuously as due to the contribution of transitions from a distribution of levels located close to the valence band [10,11,33]. In contrast, a broad defect band with a high density of states was found for charge separation across the interface SCR, probably related to the γ interlayer mentioned above. It can be concluded that the unavoidable interlayer between κ-Ga_2O_3 and the substrate is highly defective and possibly related to the defects localized at about 1.7 eV below the CB, as suggested by Fig. 11. Furthermore, a transition at 4.3 eV led to charge separation across the surface SCR and across the interface SCR. It is reasonable to assume that the transition at 4.3 eV is related to defect states 4.3 eV below E_C of κ-Ga_2O_3. This result suggests that the bump observed at about 4 eV in the PC spectrum of this polymorph can reveal a transition from a defect state to the CB partially covered by an apparent feature due to the correction to the rough PC data for the spectral irradiance (see inset of Fig. 5). However, the same

transition is not detected by CL, suggesting that it is non-radiative.

A survey of the literature was carried out in order to compare the deep levels detected in this work with the current state of knowledge. Donor states with activation energies of 1.06, 0.77 and 0.54 eV were obtained by DLTS measurements on Czochralski-grown β-Ga_2O_3 single crystals [34]. Deep defects located at 0.8, 2.04, 2.71, 3.87 and 4.3 eV below the CB edge and one level at 3.71 eV above the VB edge were found in β-Ga_2O_3 by the steady-state photo-capacitance spectroscopy technique [35]. Furthermore, dominant defect states were found at 4.4 and around 2.0…2.16 eV and states at around 0.98…1.2 eV below the CB independently of doping, and several defect peaks were observed depending on doping and growth parameters of β-Ga_2O_3 [36].

We also wish to mention that levels at E_c-0.5 and E_c-0.3 eV Ec-1.1 eV E_c-0.5 and E_v+0.47, E_v+0.8 eV, E_v+0.6 eV were reported in Ref. [37] in κ-Ga_2O_3 samples grown by different methods, undoped or slightly Sn-doped.

5. Conclusions

Complementary experimental methods were applied to study electronic transitions in β-Ga_2O_3 and κ-Ga_2O_3 epitaxial layers. SVP was particularly helpful as it allowed to distinguish between signals related to surface and interface space charge regions by illuminating the epitaxial layers from the front or from the back, across the sapphire substrate. The detected electronic transitions were compared with those extrapolated from other optical measurements, transmission, and photocurrent spectroscopies, on the same samples with as well as with data from the literature.

The effective bandgaps were evaluated at about 4.65 eV for β-Ga_2O_3 and 4.90 (near the surface) for κ-Ga_2O_3, respectively, in good agreement with other optical investigation, although some uncertainty persists because of the probable band tails related to localized states in proximity of the band edges. At the interface κ-Ga_2O_3 / substrate the bandgap was estimated to be 4.75 eV. This value, lower than the one measured at the surface, may possibly derive from a defected interlayer of an extra phase (γ). In β-Ga_2O_3, SPV signals related to defect transitions appeared at 3.5, 4.1 and 4.5 eV. In κ-Ga_2O_3, strong SPV signals related to defect transitions were observed around 1.7 eV at/near the interface whereas SPV signals were detected at 2.4 eV near the surface and at 4.3 eV near the surface and the interface. Most of the electronic transitions are consistent with features of the spectra detected by standard spectroscopies, with SPV offering the advantage of a good spatial resolution and time responses of the defects, in addition to cover energy transitions within the entire bandgap.

Author statement

The authors confirm contribution to the paper as follows: Study conception and design: Th. Dittrich; A. Parisini; M. Pavesi. Coordinator of the project and the research on Ga2O3: R. Fornari. Data collection: Th. Dittrich; M. Pavesi; A. Baraldi; F. Mezzadri; A. Sacchi; A. Parisini. Analysis and interpretation of results: Th. Dittrich; M. Pavesi; A. Baraldi; A. Parisini; F. Mezzadri. Sample deposition: M. Bosi; L. Seravalli; P. Mazzolini. Electrical contact fabrication: A. Bosio. Draft manuscript preparation: all the authors.

All authors reviewed the results and approved the final version of the manuscript.

Declaration of competing interest

The authors declare that they have no known competing financial interests or personal relationships that could have appeared to influence the work reported in this paper.

Artificial Intelligence support was not used in the writing of this manuscript.

Data availability

Data will be made available on request.

Acknowledgements

The authors would like to thank Mr. Salvatore Vantaggio for technical assistance and Dr. Francesco Mattei for his help in electrical measurements. The MOVPE epitaxial reactor for oxides was set up in 2023 with the financial support of Parma University.

Alessio Bosio, Roberto Fornari and Luca Seravalli acknowledge the financial support from PNRR MUR funded by the European Union—NextGenerationEU: project ECS_00000033_ECOSISTER "Ecosystem for Sustainable Transition in Emilia-Romagna".

Antonella Parisini acknowledges the financial support from project "MUR_DM737_A_MAFI_PARISINI DM 737 25.06.2021 - Ga2O3-based diodes for power electronics", program FIL 2021 of Parma University.

References

[1] Gallium Oxide - Technology: technology; devices and applications. Edited by S. Pearton, F. Ren, M. Mastro, 2019. Metal Oxides Series - Series Editor Ghenadii Korotcenkov.
[2] Gallium oxide: materials properties; crystal growth; and devices, Springer Nature, Springer Series in Materials Science, 2020. Editors: M. Higashiwaki, S.Fujita.
[3] B.R. Tak, S. Kumar, A.K. Kapoor, D. Wang, X. Li, H. Sun, R. Singh, Recent advances in the growth of gallium oxide thin films employing various growth techniques - a review, J. Phys. D: Appl. Phys. 54 (2021) 453002. https://pubs.acs.org/doi/10.1088/1361-6463/ac1af2.
[4] R. Fornari, M. Pavesi, V. Montedoro, D. Klimm, F. Mezzadri, I. Cora, B. Pécz, F. Boschi, A. Parisini, A. Baraldi, C. Ferrari, E. Gombia, M. Bosi, Thermal stability of ε-Ga_2O_3 polymorph, Acta Mater 140 (2017) 411–416, https://doi.org/10.1016/j.actamat.2017.08.062.
[5] F. Mezzadri, G. Calestani, F. Boschi, D. Delmonte, M. Bosi, R. Fornari, Crystal structure and ferroelectric properties of ε-Ga_2O_3 films grown on (0001)-Sapphire, Inorg. Chem. 55 (2016) 12079–12084. https://pubs.acs.org/doi/10.1021/acs.inorgchem.6b02244.
[6] I. Cora, F. Mezzadri, F. Boschi, M. Bosi, M. Čaplovičová, G. Calestani, I. Dódony, B. Pécz, R. Fornari, The real structure of ε-Ga_2O_3 and its relation to the κ-phase, Cryst. Eng. Comm. 19 (2017) 1509–1516, https://doi.org/10.1039/c7ce00123a.
[7] P. Mazzolini, Z. Fogarassy, A. Parisini, F. Mezzadri, D. Diercks, M. Bosi, L. Seravalli, A. Sacchi, G. Spaggiari, D. Bersani, O. Bierwagen, B. Moritz Janzen, M. Naomi Marggraf, M.R. Wagner, I. Cora, B. Pécz, A. Tahraoui, A. Bosio, C. Borelli, S. Leone, R. Fornari, Silane-mediated expansion of domains in Si-Doped κ-Ga_2O_3 epitaxy and its impact on the in-plane electronic conduction, Adv. Funct. Mater. 33 (2023) 2207821, https://doi.org/10.1002/adfm.202207821.
[8] S.J. Pearton, J. Yang, P.H. Cary, F. Ren, M.A. Mastro, A review of Ga_2O_3 materials; processing; and devices, Appl. Phys. Rev. 5 (2018) 011301/1-55, https://doi.org/10.1063/1.5006941.
[9] M. Pavesi, F. Fabbri, F. Boschi, G. Piacentini, A. Baraldi, M. Bosi, E. Gombia, A. Parisini, R. Fornari, ε-Ga_2O_3 epilayers as a material for solar-blind UV photodetectors, Mater. Chem. Phys. 205 (2018) 502–507, https://doi.org/10.1016/j.matchemphys.2017.11.023.
[10] V. Montedoro, A. Torres, S. Dadgostar, J. Jimenez, M. Bosi, A. Parisini, R. Fornari, Cathodoluminescence of undoped and Si-doped ε-Ga_2O_3 films, Mat. Sci. Eng. B 264 (2021) 114918/1-7, https://doi.org/10.1016/j.mseb.2020.114918.
[11] A. Parisini, A. Bosio, H.J. von Bardeleben, J. Jimenez, S. Dadgostar, M. Pavesi, A. Baraldi, S. Vantaggio, R. Fornari, Deep and shallow electronic states associated to doping, contamination and intrinsic defects in ε-Ga_2O_3 epilayers, Mat. Sci. in Semicond. Processing 138 (2022) 106307, https://doi.org/10.1016/j.mssp.2021.106307.
[12] L. Kronik, Y. Shapira, Surface photovoltage phenomena: theory, experiment, and applications, Surf. Sci. Rep. 37 (1999) 1, https://doi.org/10.1016/S0167-5729(99)00002-3.
[13] T. Dittrich, S. Fengler, Surface Photovoltage Analysis of Photoactive Materials, World Scientific Publishing Europe Ltd., London, UK, 2020.
[14] Th. Dittrich, L.E. Valle Rios, S. Kapil, G. Guireva, N. Rujisamphan, S. Schorr, Temperature dependent transient surface photovoltage spectroscopy of a $Cu_{1.95}Zn_{1.1}Sn_{0.96}Se_4$ kesterite single phase powder, Appl. Phys. Lett. 110 (2017) 023901, https://doi.org/10.1063/1.4973539.
[15] S. Fengler, H. Kriegel, M. Schieda, H. Gutzmann, T. Klassen, M. Wollgarten, Th. Dittrich, Charge transfer in c-Si(n^{++})/TiO_2(ALD) at the amorphous/anatase transition: a transient surface photovoltage spectroscopy study, ACS Appl. Mater. Interfaces 12 (2020) 3140–3149, https://doi.org/10.1021/acsami.9b17592.
[16] I. Levine, A. Al-Ashouri, A. Musiienko, H. Hempel, A. Magomedov, A. Drevilkauskaite, V. Getautis, D. Menzel, K. Hinrichs, T. Unold, S. Albrecht, Th. Dittrich, Charge transfer rates and electron trapping at buried interfaces of perovskite solar cells, Joule 5 (2021) 2915–2933, https://doi.org/10.1016/j.joule.2021.07.016.

[17] T. Dittrich, S. Fengler, N. Nickel, Surface Photovoltage spectroscopy over wide time domains for semiconductors with ultrawide bandgap: example of gallium oxide, Phys. Status Solidi A 218 (2021) 2100167/1-11, https://doi.org/10.1002/pssa.202100167.
[18] Th. Dittrich, Transient surface photovoltage spectroscopy of diamond, AIP Adv 12 (2022) 065206, https://doi.org/10.1063/5.0089398.
[19] M. Bosi, P. Mazzolini, L. Seravalli, R. Fornari, Ga_2O_3 polymorphs: tailoring the epitaxial growth conditions, J. Mater. Chem. C 8 (2020) 10975. https://pubs.rsc.org/en/content/articlelanding/2020/TC/D0TC02743J.
[20] M. Bosi, L. Seravalli, P. Mazzolini, F. Mezzadri, R. Fornari, Thermodynamic and kinetic effects on the nucleation and growth of ε/κ- or β-Ga_2O_3 by metal–organic vapor phase epitaxy, Cryst. Growth Des. 21 (2021) 6393–6401, https://doi.org/10.1021/acs.cgd.1c00863.
[21] J.E.N. Swallow, J.B. Varley, L.A.H. Jones, J.T. Gibbon, L.F.J. Piper, V.R. Dhanak, T. D. Veal, Transition from electron accumulation to depletion at β-Ga_2O_3 surfaces: the role of hydrogen and the charge neutrality level, APL Mater 7 (2019) 022528, https://doi.org/10.1063/1.5054091.
[22] C. Borelli, A. Bosio, A. Parisini, M. Pavesi, S. Vantaggio, R. Fornari, Electronic properties and photo-gain of UV-C photodetectors based on high-resistivity orthorhombic κ-Ga_2O_3 epilayers, Mat. Sci. Eng. B 286 (2022) 116056, https://doi.org/10.1016/j.mseb.2022.116056.
[23] J. Klein, L. Kampermann, B. Mockenhaupt, M. Behrens, J. Strunk, G. Bacher, Limitations of the Tauc plot method, Adv. Funct. Mater. 33 (2023) 2304523, https://doi.org/10.1002/adfm.202304523.
[24] K. Ghosh, U. Singisetti, Ab initio velocity-field curves in monoclinic β-Ga_2O_3, J. Appl. Phys. 122 (2017) 035702, https://doi.org/10.1063/1.4986174.
[25] P.R. Jubu, F.K. Yam, V.M. Igba, K.P. Beh, Tauc-plot scale and extrapolation effect on bandgap estimation from UV–vis–NIR data – a case study of β-Ga_2O_3, J. Solid State Chem. 290 (2020) 121576, https://doi.org/10.1016/j.jssc.2020.121576.
[26] A. Dolgonos, T.O. Mason, K.R. Poeppelmeier, Direct optical bandgap measurement in polycrystalline semiconductors: a critical look at the Tauc method, J. Solid State Chem. 240 (2016) 43, https://doi.org/10.1016/j.jssc.2016.05.010.
[27] A.R. Zanatta, Revisiting the optical bandgap of semiconductors and the proposal of a unified methodology to its determination, Sci. Rep. 9 (2019) 11225, https://doi.org/10.1038/s41598-019-47670-y.
[28] T. Gake, Y. Kumagai, F. Oba, First-principles study of self-trapped holes and acceptor impurities in Ga_2O_3 polymorphs, Phys. Rev. Materials 3 (2019) 044603, https://doi.org/10.1103/PhysRevMaterials.3.044603.
[29] Y. Xu, J.-H. Park, Z. Yao, C. Wolverton, M. Razeghi, J. Wu, V.P. Dravid, Strain-induced metastable phase stabilization in Ga_2O_3 thin films, ACS Appl. Mater. Interfaces 11 (2019) 5536–5543, https://doi.org/10.1021/acsami.8b17731.
[30] K. Jiang, J. Tang, M.J. Cabral, A. Park, L. Gu, R.F. Davis, L.M. Porter, Layered phase composition and microstructure of κ-Ga_2O_3-dominant heteroepitaxial films grown via MOCVD, J. Appl. Phys. 131 (2022) 055305, https://doi.org/10.1063/5.0073517.
[31] L.E. Ratcliff, T. Oshima, F. Nippert, B.M. Janzen, E. Kluth, R. Goldhahn, M. Feneberg, P. Mazzolini, O. Bierwagen, C. Wouters, M. Nofal, M. Albrecht, J.E. N. Swallow, L.A.H. Jones, P.K. Thakur, T.-L. Lee, C. Kalha, C. Schlueter, T.D. Veal, J.B. Varley, M.R. Wagner, A. Regou, Tackling disorder in γ-Ga_2O_3, Adv. Mater. 34 (2022) 2204217, https://doi.org/10.1002/adma.202204217.
[32] R. Schewski, G. Wagner, M. Baldini, Z. Galazka, D. Gogova, T. Schulz, T. Remmele, T. Markurt, H. von Wenckstern, M. Grundmann, O. Bierwagen, P. Vogt, M. Albrecht, Epitaxial stabilization of pseudomorphic α-Ga_2O_3 on sapphire (0001), Appl. Phys. Express 8 (2015) 011101, https://doi.org/10.7567/APEX.8.011101.
[33] M. Mulazzi, F. Reichmann, A. Becker, W.M. Klesse, P. Alippi, V. Fiorentini, A. Parisini, M. Bosi, R. Fornari, The electronic structure of ε-Ga_2O_3, APL Mater 7 (2019) 022522/1-6, https://doi.org/10.1063/1.5054395.
[34] K. Irmscher, Z. Galazka, M. Pietsch, R. Uecker, R. Fornari, Electrical properties of β-Ga_2O_3 single crystals grown by the Czochralsky method, Appl. Phys. 110 (2011) 063720, https://doi.org/10.1063/1.3642962.
[35] Y. Nakano, Electrical characterization of β-Ga_2O_3 single crystal substrates, J. Sol. State Sci. Technol. 6 (2017) P615, https://doi.org/10.1149/2.0181709jss.
[36] H. Ghadi, J.F. McGlone, C.M. Jackson, E. Farzana, Z. Feng, A.F.M. Anhar Uddin Bhuiyan, H. Zhao, A.R. Arehart, S.A. Ringel, Full bandgap defect state characterization of β-Ga_2O_3 grown by metal organic chemical vapor deposition, APL Mater 8 (2020) 021111, https://doi.org/10.1063/1.5142313.
[37] A. Polyakov, I.-H. Lee, V. Nikolaev, A. Pechnikov, A. Miakonkikh, M. Scheglov, E. Yakimov, A. Chikiryaka, A. Vasilev, A. Kochkova, I. Shchemerov, A. Chernykh, S. Pearton, Properties of κ-Ga_2O_3 prepared by epitaxial lateral overgrowth, Adv. Mater. Interfaces (2023) 2300394, https://doi.org/10.1002/admi.202300394.